



Characterization of polycyclic aromatic hydrocarbon (PAHs) source profiles in urban PM_{2.5} fugitive dust: A large-scale study for 20 Chinese cities

Xuesong Gong^{a,b}, Zhenxing Shen^{a,b,c,*}, Qian Zhang^d, Yaling Zeng^a, Jian Sun^a, Steven Sai Hang Ho^e, Yali Lei^a, Tian Zhang^a, Hongmei Xu^a, Song Cui^c, Yu Huang^b, Junji Cao^b

^a Department of Environmental Science and Engineering, Xi'an Jiaotong University, Xi'an 710049, China

^b Key Lab of Aerosol Chemistry & Physics, SKLLQG, Institute of Earth Environment, Chinese Academy of Sciences, Xi'an, China

^c International Joint Research Center for Persistent Toxic Pollutants, School of Water Conservancy and Civil Engineering, Northeast Agricultural University, Harbin 150030, China

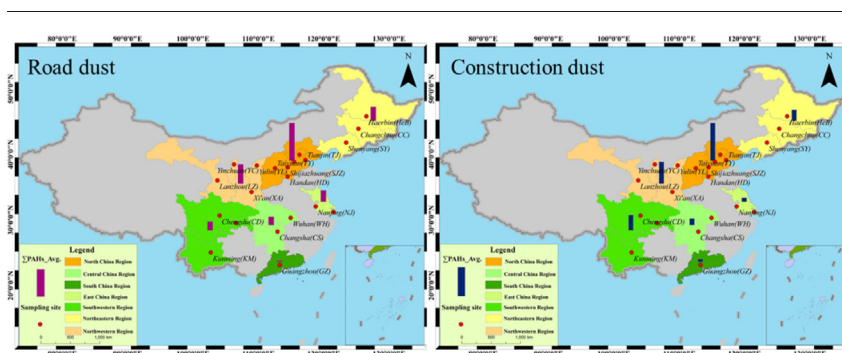
^d School of Environmental & Municipal Engineering, Xi'an University of Architecture and Technology, Xi'an 710055, China

^e Division of Atmospheric Sciences, Desert Research Institute, Reno, NV 89512, United States

HIGHLIGHTS

- PAHs source profiles in urban fugitive dust PM_{2.5} samples were investigated in 20 Chinese cities.
- The differences of ΣPAHs between road dust (RD) and construction dust (CD) were much larger in southern and east regions.
- The ΣPAHs for RD displayed a pattern of “high in northern and low in southern”.

GRAPHICAL ABSTRACT



ARTICLE INFO

Article history:

Received 22 April 2019

Received in revised form 5 June 2019

Accepted 6 June 2019

Available online 8 June 2019

Editor: Jianmin Chen

Keywords:

Urban fugitive dust

Polycyclic aromatic hydrocarbons (PAHs)

Source identification

Health risk evaluation

Chinese cities

ABSTRACT

Polycyclic aromatic hydrocarbons (PAHs) in road dust (RD) and construction dust (CD) in PM_{2.5} were quantified in the samples collected in 20 Chinese cities. The PAHs profiles in urban PM_{2.5} fugitive dusts were determined and their potential health risks were evaluated. Seven geographical regions in China were identified as northwest China (NWC), the North China Plain (NCP), northeast China (NEC), central China (CC), south China (SC), southwest China (SWC), and east China (EC). The overall average concentrations of total quantified PAHs (ΣPAHs) were 23.2 ± 18.9 and $22.8 \pm 29.6 \mu\text{g} \cdot \text{g}^{-1}$ in RD and CD of PM_{2.5}, indicating that severe PAHs pollution to urban fugitive dusts in China. The differences of ΣPAHs between RD and CD were minor in northern and central regions of China but much larger in southern and east regions. The ΣPAHs for RD displayed a pattern of “high in northern and low in southern”, and characterized by large abundance of high molecular weights (HMWs) PAHs, indicating that vehicle emission was the predominant pollution origin. Additionally, higher diagnostic ratios of fluoranthene/(fluoranthene + pyrene) in NCP, CC, and SWC suggest critical contributions of biomass burning and coal combustion for RD in these areas. In comparison, gasoline combustion was the major pollution source for CD PAHs in NWC, NCP, NEC, and CC, whereas industrial emissions such as cement production and iron smelting had strong impacts in the heavy industrial regions. The total benzo[a]pyrene (BaP) carcinogenic potency concentrations (BaP_{TEQ}) for RD and CD both showed the lowest in SC (0.05 and 0.07, respectively) and

* Corresponding author at: Department of Environmental Science and Engineering, Xi'an Jiaotong University, Xi'an 710049, China.
E-mail address: zxshen@mail.xjtu.edu.cn (Z. Shen).

the highest in NCP (10.99 and 7.67, respectively). The highest and lowest incremental life cancer risks (ILCR) were found in NCP and SC, coinciding with the spatial distributions of ambient PAHs levels. The total CD-related cancer risks for adults and children ($\sim 10^{-4}$) suggest high potential health risks in NCP, SWC, and NWC, whereas the evaluated values in EC and SC indicate virtual safety ($\leq 10^{-6}$).

© 2019 Elsevier B.V. All rights reserved.

1. Introduction

Fugitive dust is a major fraction of particulate matter (PM) that originates from a variety of open sources, such as paved and unpaved roadways, vehicular track-out, non-vegetated areas, material storage piles, and construction-related activities (Amato et al., 2011; Bhaskar and Sharma, 2008; Cao et al., 2008; Diego et al., 2009; Zhang et al., 2014). It is the most prevalent component in urban PM (Yu et al., 2013; Chen et al., 2007; Ajmone-Marsan et al., 2008). According to the statistic, fugitive dust accounts for ~20% of PM with aerodynamic diameters $< 2.5 \mu\text{m}$ ($\text{PM}_{2.5}$) in most Chinese cities (Cao et al., 2012). Due to its heterogeneous origins, fugitive dust composites of a complex organic and inorganic mixture on outdoor ground surfaces. The mixture can physically contribute to atmospheric pollution through resuspension and transportation. Quantities and compositions of inorganic and organic materials, such as elements, ions, and carbon fractions, in $\text{PM}_{2.5}$ were often measured to evaluate adverse effects and to conduct source apportionments (Cao et al., 2008; Shen et al., 2016; Zhang et al., 2014; Sun et al., 2019). Comparatively, important toxic organic contaminants of polycyclic aromatic hydrocarbons (PAHs) in $\text{PM}_{2.5}$ fugitive dust have not been thoroughly discussed.

Numerous epidemiological studies confirmed that PAHs are a critical class of organic pollutants in fugitive dust formed from incomplete combustion or pyrolysis of organic materials (Hussain et al., 2015; Manoli et al., 2004; Han et al., 2009; Wang et al., 2018; Zeng et al., 2018). Additionally, 16 PAHs have been identified as priority control pollutants by the United States Environmental Protection Agency (U.S.EPA) due to their health impacts. Both short-term and long-term exposures to particular PAHs, including benz[a]anthracene, benzo[a]pyrene, benzo[b]fluoranthene, benzo[j]fluoranthene, benzo[k]fluoranthene, chrysene, dibenz[a,h]anthracene, and indeno[1,2,3-c,d]pyrene, can impair lung function and even cause cancer (Kim et al., 2013; Diggs et al., 2011). The importance of PAHs in fugitive dust has been widely recognized. The concentration and chemical composition of PAHs in fugitive dust were greatly affected by anthropogenic activities, including the emissions from local transportation, industry and even air pollution transmission and deposition (Yang et al., 1999; Murakami et al., 2005; Han et al., 2009). The concentrations of PAHs in fugitive dust vary greatly depending on geographical location, energy infrastructure, and urban pollution. The concentrations of PAHs in $\text{PM}_{2.5}$ fugitive dust in an industrial city in Korea (Lee and Dong, 2011) were 2–8 times higher than those collected in Delhi, India (Agarwal et al., 2009), Birmingham, UK (Smith et al., 1995), and Niteroi, Brazil (Netto et al., 2006). Previous studies revealed that fugitive dust PAHs in urban areas mainly originate from cooking, smoking, mining, metal working, and oil refining (Kong et al., 2015; Martuzevicius et al., 2011; Han et al., 2009; Iwegbue and Obi, 2016; Lannerö et al., 2008; Armstrong et al., 2004; See et al., 2006).

Due to rapid urbanization in recent decades, the numbers of construction work and traffic flow have been increasing in most Chinese urban cities that have considerably stressed the environments, particularly causing contaminations on fugitive dusts. Construction sites and roadways are hot-spot sources for urban fugitive fine-particle PAHs, and their pollution levels and health impacts should be investigated. In this study, PAHs profiles in $\text{PM}_{2.5}$ fugitive dusts were investigated in 20 Chinese cities, where can be defined as seven regions (northwest China [NWC], the North China Plain [NCP], northeast China [NEC], central China [CC], south China [SC], southwest China [SWC], and east China [EC]) of the country. The objectives of this study are 1) to

investigate the PAHs profiles in $\text{PM}_{2.5}$ fugitive dust over 20 Chinese cities; 2) to identify the potential pollution sources for both road dust (RD) and construction dust (CD), and 3) to evaluate the potential toxicological impacts and cancer risks for adults and children.

2. Materials and methods

2.1. Sample locations and collections

Urban fugitive dust $\text{PM}_{2.5}$ samples were collected in 20 Chinese cities across seven regions, including (i) NWC: Xi'an, Lanzhou, and Yinchuan; (ii) the NCP: Beijing, Tianjin, Baoding, Shijiazhuang, Handan, and Taiyuan; (iii) NEC: Harbin, Changchun, and Shenyang; (iv) CC: Wuhan and Changsha; (v) SC: Guangzhou; (vi) SWC: Chongqing, Chengdu, and Kunming; and (vii) EC: Nanjing and Shanghai (Fig. 1). According to geography, the NWC, NCP, NEC, and CC were grouped as northern and central regions of China, and SC, SWC, and EC were considered as southern region. The regional definition was consistent with previous study shown in Sun et al. (2019), in which the source profiles of elements, ionic species, and carbonaceous species in urban fugitive dust $\text{PM}_{2.5}$ were reported.

A total of 180 sets of road dust (RD) and construction dust (CD) samples were collected in the 20 cities on non-rainy days from March 2014 to July 2015. The dust samples were collected through in-situ resuspension; that is, the dust on the ground surface was manually swept using a broom by our technical staff, simulating the work of road cleaners. RD samples were mainly collected from urban major streets and small streets, and the collection of construction dust was mainly from various types of building sites, including residential and factory construction sites. $\text{PM}_{2.5}$ mini-volume samplers (Airmetrics, Springfield, Oregon, USA) were employed at a flow rate of $5 \text{ L} \cdot \text{min}^{-1}$ to collect the dust $\text{PM}_{2.5}$. Sampling times ranged from 30 to 60 min depending on the real dust loading at each sampling site. At each site, one set of $\text{PM}_{2.5}$ sample was collected on 47-mm-diameter Teflon membrane filters ($\text{PM}_{2.5}$ Air Monitoring Polytetrafluoroethylene Filters, Whatman Limited, Maidstone, UK) for mass measurement and elemental analysis, and another set was collected on 47-mm Whatman quartz microfiber filters for ionic and carbonaceous species (including PAHs) analyses. The detailed sampling procedures were referred to Shen et al. (2016) and Sun et al. (2019).

2.2. PAHs extraction and measurement

A quarter of each aerosol filter sample was Soxhlet-extracted using 200 mL of dichloromethane (DCM) for 24 h, and concentrated into 1 mL using a rotary evaporator. Subsequently, each extract was separated through flash column filled with silica gel. The extract was washed using 20 mL of hexane and subsequently eluted using a 15-mL mixture of hexane and DCM (1:1 by volume). The eluent was evaporated to 1 mL and blown down to 0.5 mL under a gentle nitrogen stream at 60°C . The extract was finally transferred into ampoule bottles and stored in a refrigerator until analysis.

Ten target U.S.EPA priority PAHs, including phenanthrene (Phe, 3-ring), anthracene (Ant, 3-ring), fluoranthene (Fla, 4-ring), pyrene (Pyr, 4-ring), benzo[a]fluoranthene (BaA, 4-ring), chrysene (Chr, 4-ring), benzo[b]fluoranthene (Bbflu, 5-ring), benzo[k]fluoranthene (Bkflu, 5-ring), benzo[a]pyrene (BaP, 6-ring) and benzo[ghi]perylene (BghiP, 6-ring), dibenz[a,h]anthracene (DahA, 6-ring), and indeno

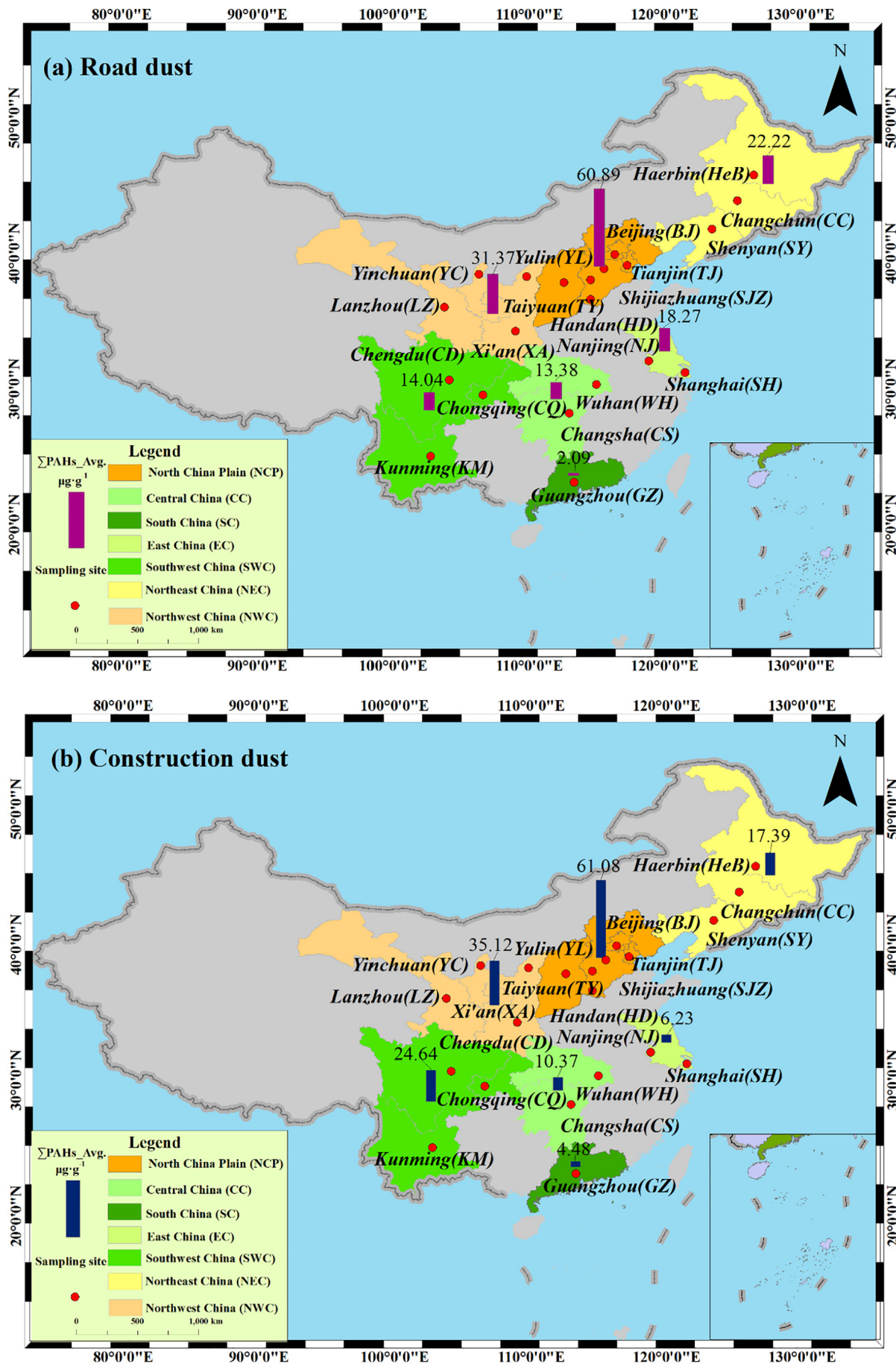


Fig. 1. Maps show the division of seven regions and the averages of ΣPAHs for (a) road and (b) construction dust (indicated by bar height).

[1,2,3-cd]pyrene (IND) (IndP, 6–ring), in the extracts were quantified using Agilent 6890 gas chromatograph (GC)/5975 mass spectrometer (MS) (Agilent Technology, Santa Clara, CA, USA). The extraction recoveries for the target PAHs was in a range of 70–120%. Phenanthrene-D10 and perylene-D12 were added and served as internal standards (IS) to monitor the performance and matrix effects. The recoveries of phenanthrene-D10 and perylene-D12 were 66–109% and 76–122%, respectively. Detailed analytical and quality control procedures were shown in our publication (Wang et al., 2018).

2.3. Data analysis

2.3.1. Coefficient of divergence

The coefficient of divergence (CoD), a self-normalizing parameter, was adopted to compare the spread of the average concentrations of PAHs among different regions. The CoD was calculated as follows:

$$CoD_{jk} = \sqrt{\frac{1}{p} \sum_{i=1}^p \left(\frac{x_{ij} - x_{ik}}{x_{ij} + x_{ik}} \right)^2} \quad (1)$$

where j and k represent the two profiles of the sampling sites; p is the number of investigated ten target PAHs in this study; and x_{ij} and x_{ik} represent the average mass concentrations of PAH species i for j and k , respectively. If CoD_{jk} approaches zero, then the PAH composition profiles are similar; if it approaches one, then the profiles are significantly different (Zhang et al., 2014; Shen et al., 2016).

2.3.2. Assessment of health risk from PAHs exposure

The human exposure risk to the PAHs in the dusts was evaluated using benzo[a]pyrene toxic equivalency (TEQ) and incremental lifetime cancer risk (ILCR) factors. The risks for the target PAHs have been evaluated in previous studies according to the BaP carcinogenic (BaP_{TEQ}) measurement. In this study, BaP_{TEQ} of the PAHs was calculated using the following equation:

$$\sum BaP_{TEQ} = \sum (C_i \times TEQ_i) \quad (2)$$

where BaP_{TEQ} is the cancer potency relative to BaP, and C_i is the individual PAH concentration. The TEQ values of the seven carcinogenic PAHs were BaP (1), BaA (0.1), Bbflu (0.1), Bkflu (0.01), Chr (0.001), DahA (1), and IndP (0.1) (US EPA, 1993; Durant et al., 1996). The guideline value of BaP_{TEQ}, estimated by the Canadian Council of Ministers of the Environment to be $0.1 \mu\text{g} \cdot \text{g}^{-1}$, and thus the BaP_{TEQ} > $0.1 \mu\text{g} \cdot \text{g}^{-1}$ represented high carcinogenicity.

Based on the U.S.EPA standard models, the ILCRs were divided into three categories: ingestion (ILCR_{ingestion}), dermal contact (ILCR_{dermal}), and inhalation (ILCR_{inhalation}). These ILCRs were calculated for the urban fugitive dust PAH concentrations in each sample as follows:

$$ILCR_{ingestion} = \frac{CS \times \left(CSF_{ingestion} \times \sqrt[3]{\left(\frac{BW}{70} \right)} \right) \times IR_{ingestion} \times EF \times ED}{BW \times AT \times 10^6} \quad (3)$$

$$ILCR_{dermal} = \frac{CS \times \left(CSF_{dermal} \times \sqrt[3]{\left(\frac{BW}{70} \right)} \right) \times SA \times AF \times ABS \times EF \times ED}{BW \times AT \times 10^6} \quad (4)$$

$$ILCR_{inhalation} = \frac{CS \times \left(CSF_{inhalation} \times \sqrt[3]{\left(\frac{BW}{70} \right)} \right) \times IR_{inhalation} \times EF \times ED}{BW \times AT \times PEF} \quad (5)$$

where CS is the sum of converted PAHs concentrations based on the toxic equivalents of BaP using the TEQ (Nisbet and LaGoy, 1992); CSF

is carcinogenic slope factor ($\text{mg} \cdot \text{kg}^{-1} \cdot \text{day}^{-1}$)⁻¹; BW is body weight (kg); AT is average life span (years); EF is exposure frequency ($\text{day} \cdot \text{year}^{-1}$); ED is exposure duration (years); $IR_{inhalation}$ is the inhalation rate ($\text{m}^3 \cdot \text{day}^{-1}$); $IR_{ingestion}$ is the soil intake rate ($\text{mg} \cdot \text{day}^{-1}$); SA is the dermal surface exposure (cm^2); AF is the dermal adherence factor ($\text{mg} \cdot \text{cm}^{-2} \cdot \text{h}^{-1}$); ABS is the dermal adsorption fraction; and PEF is the particle emission factor ($\text{m}^3 \cdot \text{kg}^{-1}$). These parameters used in the models for children (1–6 years old) and adults (7–31 years old) were based on the Risk Assessment Guidelines established by the U.S.EPA and related publications, which were listed by Wang et al. (2011). The values of CSF_{ingestion}, CSF_{dermal}, and CSF_{inhalation} of BaP were 7.3, 25, and $3.85 (\text{mg} \cdot \text{kg}^{-1} \cdot \text{day}^{-1})^{-1}$, respectively, according to the cancer-causing ability of BaP (Peng et al., 2011).

3. Results and discussion

3.1. Spatial distribution of PAHs in urban PM_{2.5} fugitive dust

The total concentrations of target PAHs (\sum PAHs) in the RD and CD PM_{2.5} samples collected in the seven Chinese regions were showed in Fig. 1. The levels of \sum PAHs_{RD} varied from 2.09 to $81.22 \mu\text{g} \cdot \text{g}^{-1}$ with a geometric mean of $21.59 \mu\text{g} \cdot \text{g}^{-1}$. In contrast, the \sum PAHs_{CD} ranged from 0.38 to $106.34 \mu\text{g} \cdot \text{g}^{-1}$ with an average of $22.82 \mu\text{g} \cdot \text{g}^{-1}$. The results illustrate that the PAHs were more abundant in Chinese fugitive dust, compared with those of Dhanbad, India ($3.5 \mu\text{g} \cdot \text{g}^{-1}$) (Suman et al., 2016), Niteroi City, Brazil ($0.8 \mu\text{g} \cdot \text{g}^{-1}$) (Netto et al., 2006), and California, U.S. ($0.8 \mu\text{g} \cdot \text{g}^{-1}$) (Rogge et al., 2007).

With regards to geographic distribution, the mean \sum PAHs_{RD} were shown in a decreasing order of NCP ($60.9 \mu\text{g} \cdot \text{g}^{-1}$) > NWC ($31.4 \mu\text{g} \cdot \text{g}^{-1}$) > NEC ($22.2 \mu\text{g} \cdot \text{g}^{-1}$) > EC ($18.3 \mu\text{g} \cdot \text{g}^{-1}$) > SWC ($14.0 \mu\text{g} \cdot \text{g}^{-1}$) > CC ($13.4 \mu\text{g} \cdot \text{g}^{-1}$) > SC ($2.1 \mu\text{g} \cdot \text{g}^{-1}$). In summary, the PM_{2.5} \sum PAHs_{RD} were higher in the northern than the southern Chinese cities. This can be attributed to the accumulations from the prevalence of crustal erosion, heating activities, and emissions from heavy industries in the northern regions (Cao et al., 2012; Majumdar et al., 2012). The spatial distribution of \sum PAHs_{CD} was slightly different from \sum PAHs_{RD}, while higher value was found in SWC than NEC. The highest \sum PAHs_{CD} ($60.9 \mu\text{g} \cdot \text{g}^{-1}$) and \sum PAHs_{RD} ($61.1 \mu\text{g} \cdot \text{g}^{-1}$) were both seen in NCP which were >20 and >10 times of those in SC (\sum PAHs_{CD} = $2.1 \mu\text{g} \cdot \text{g}^{-1}$; \sum PAHs_{RD} = $4.5 \mu\text{g} \cdot \text{g}^{-1}$).

The concentrations varied considerably among the cities, even in the same region, due to influences by emission quantities and meteorological conditions. This was particularly obvious in northern China. As presented in Table S1, the NWC cities of XA, YC, and LZ exhibited relatively high \sum PAHs_{RD} (i.e., > $20 \mu\text{g} \cdot \text{g}^{-1}$), whereas much lower value was seen in YL ($5.32 \mu\text{g} \cdot \text{g}^{-1}$). High \sum PAHs_{RD} should coincide with the high PAHs in airborne PM. In fact, high ambient PM_{2.5} PAHs concentration was reported in Xi'an (XA) (Wang et al., 2018; Zeng et al., 2018). The lower value was seen at Yulin (YL) because it is located in the Mu Us desert margin, where is less influenced by traffic in this noncapital city. The distribution of \sum PAHs_{CD} generally differed from that of \sum PAHs_{RD}. The highest \sum PAHs_{CD} value was seen in XA ($69.0 \mu\text{g} \cdot \text{g}^{-1}$) but much low \sum PAHs_{CD} values were reported in other NWC cities (10.16 – $13.17 \mu\text{g} \cdot \text{g}^{-1}$). This can be explained by the fact that Xi'an (XA) has re-emerged as an industrial center in NWC (Zhang et al., 2014). In the NCP region, \sum PAHs_{RD} and \sum PAHs_{CD} in Baoding (BD) were as high as 81.2 and $106.3 \mu\text{g} \cdot \text{g}^{-1}$, respectively, followed by those of Taiyuan (TY) (58.7 and $96.6 \mu\text{g} \cdot \text{g}^{-1}$, respectively). These two are widely known as heavy coal and steel industrial cities. In southern China, the lowest \sum PAHs_{RD} was seen in Guangzhou (GZ). In this study, the ratios of RD to CD were consistent and individually approached to unity in the northern and central Chinese regions, including NWC (0.8), NCP (0.9), NEC (1.3), and CC (1.2). This finding indicates that construction-related activities and vehicle emissions simultaneously elevated the abundance of PAHs in urban fugitive dust. However, the variations on RD/CD values in the eastern and southern Chinese regions were

considerably greater, ranging from 0.47 (SC) to 2.93 (EC). These may reflect that more industrial and construction-related emissions were abundant in EC regions.

3.2. Differences of PAHs in road and construction dusts

The distributions of combustion-derived PAHs (abbreviated as COM-PAHs) including Fla, Pyr, Chr, Bbflu, Bkflu, BaA, BaP, and BghiP are plotted in Fig. 2a and b. The ratios of $\sum \text{COM-PAHs}_{\text{RD}}$ to $\sum \text{PAHs}_{\text{RD}}$ ranged from 39.7% to 90.8%, with an average of 65.5%. Additionally, the ratio showed the trend of $\text{NCP} > \text{NWC} > \text{NEC} > \text{EC} > \text{CC} > \text{SWC} > \text{SC}$, suggesting that the combustion sources in northern China were the greater contributors of PAHs than those in southern China. For CD, $\sum \text{COM-PAHs}_{\text{CD}}$ in NCP, NWC, SWC, and NEC were more abundance than that in other regions. These results are partially supported by Lin and Wang (2014), which reported that NCP (i.e., Hebei), NEC (i.e., Liaoning), and NWC (i.e., Shanxi) were the top three regions in crude steel production in China.

As illustrated in Fig. 2c and d, the concentration of BghiP was the most abundant PAH in RD samples collected in most cities which were 1.2–4 times higher than that in CD samples, demonstrating that vehicle emission significantly contributed to PAHs in RD (Wu et al., 2014; Kong et al., 2015). High levels of Pyr and Phe were also detected, emphasizing the strong influence of diesel emissions (Jang et al., 2013). In both of RD and CD samples, Fla comprised a substantial fraction (5%–35%). Fla is a biomass burning indicator; thus, our finding indicates the relatively high contribution of biomass burning to urban fugitive dust in China (bin Abas et al., 1995; Chen et al., 2014). Regarding to geographic distribution, both CD and RD samples collected in NWC region exhibited relatively high concentrations of BghiP, probably ascribed to the emissions from the heavy-duty diesel vehicles for construction works in this region. In addition, Pyr, Chr, and BbF were the major species in the fugitive dust $\text{PM}_{2.5}$ samples in the NCP and NWC regions. These PAHs are known

as indicators of emissions from coal burning (Lima et al., 2005). Furthermore, B(b + k)flu are indicators of iron smelting and coal burning, considerably differed between the samples collected in northern and southern China (Kong et al., 2013; Yang et al., 2002; Lima et al., 2005). Therefore, the overall findings verify that heavy industrial activities contributed to PAHs in urban dusts in northern China, consistent with the energy infrastructure and consumption in this region.

CoD values were calculated among the five regions to further investigate the difference between RD and CD PAHs profiles (Fig. 3). CoD for EC and SC were not calculated because only few PAHs were above the detection limits in the two regions. Generally, the calculated CoD values were high (>0.21) (Fig. 3a), indicating that the compositions of PAHs were dissimilar across the urban areas. The highest value was seen in SWC (0.36; Fig. 3f), revealing that PAHs in CD differed considerably from RD in this region, mainly driven by BghiP, B(b + k)flu, and Chr. It was noted that the higher compositions of BghiP in the RD samples were found, implying the important contribution of vehicle emissions at SWC. In contrast, higher concentrations of B(b + k)flu and Chr in CD confirmed the influence of coal-related industrial activities. The next highest CoD value was found in NEC (0.29), where higher mass composition of Chr in CD reflected a mix of pollutions from vehicle emissions and coal combustion. In NWC, the high mass composition of BbF in CD suggested the strong influence of biomass burning. By contrast, lower CoD values (NCP:0.17; CC:0.14) were reported in NCP and CC.

3.3. Distribution of PAHs based on number of aromatic rings

As illustrated in Fig. 4, more than four-rings PAHs (include four-rings) were dominant in both urban RD and CD profiles. These findings suggest a strong combustion origin for PAHs in Chinese urban fugitive dust $\text{PM}_{2.5}$ (Zakaria et al., 2002). The PAHs profiles for RD were dominated by five-to-six rings PAHs, accounted for approximately 50% of

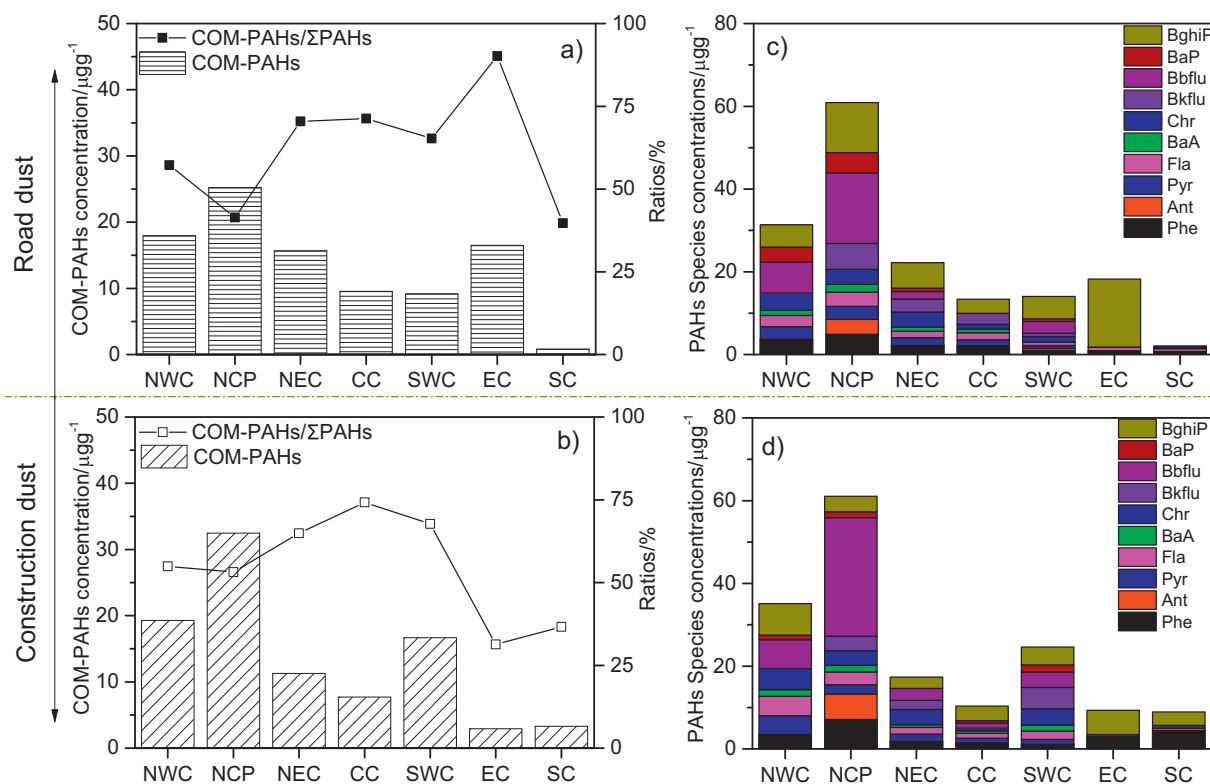


Fig. 2. a) and b) Combustion-PAHs (COM-PAHs) and their ratio to ΣPAHs for the road and construction dusts; the right scale shows mass concentrations and the left scale shows mass percentages; c) and d) mass concentration of individual PAHs in $\text{PM}_{2.5}$ for road and construction dusts.

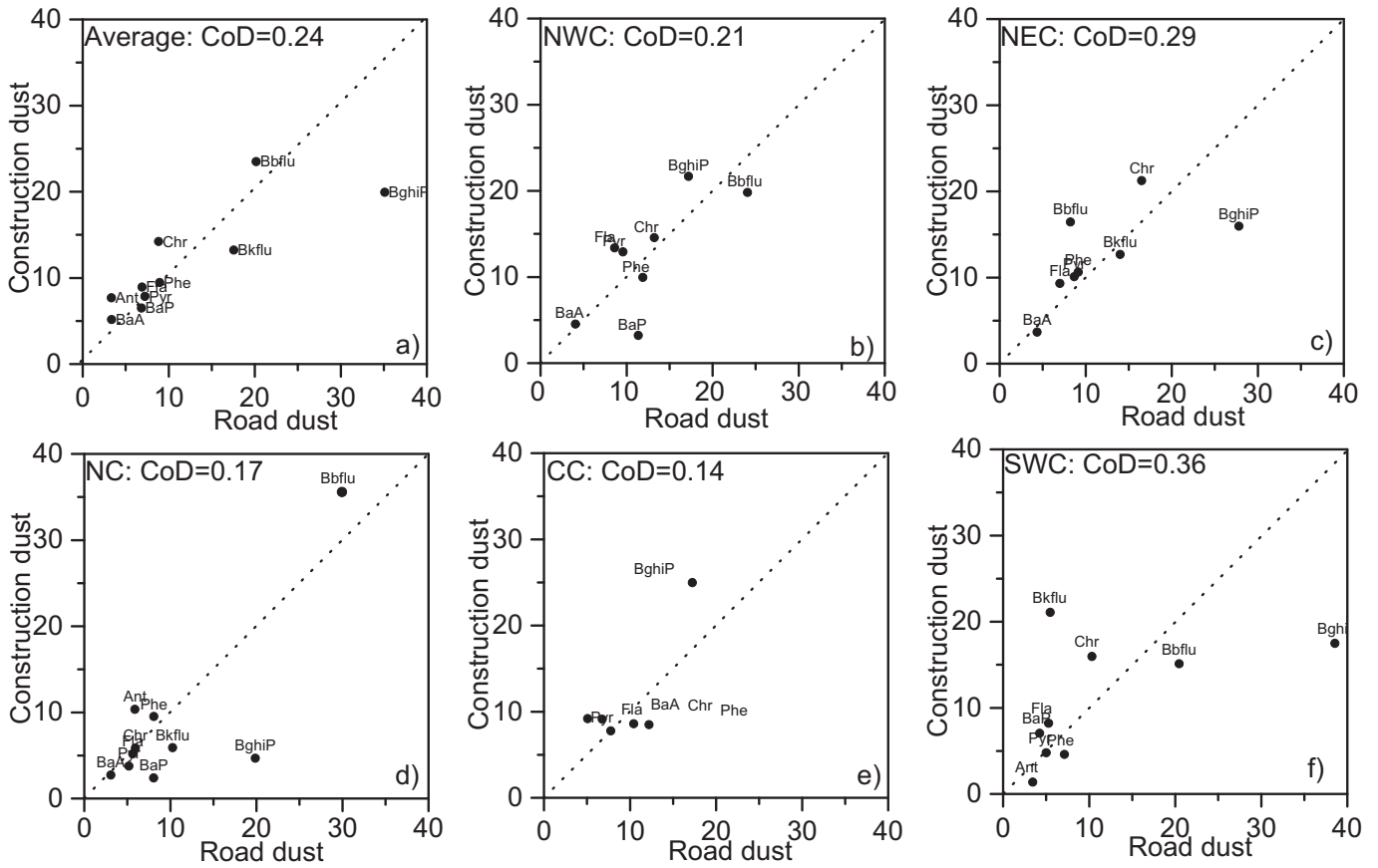


Fig. 3. Comparison of PAH mass percentages for the road and construction dusts over five regions in China. CoD represents coefficient of divergence.

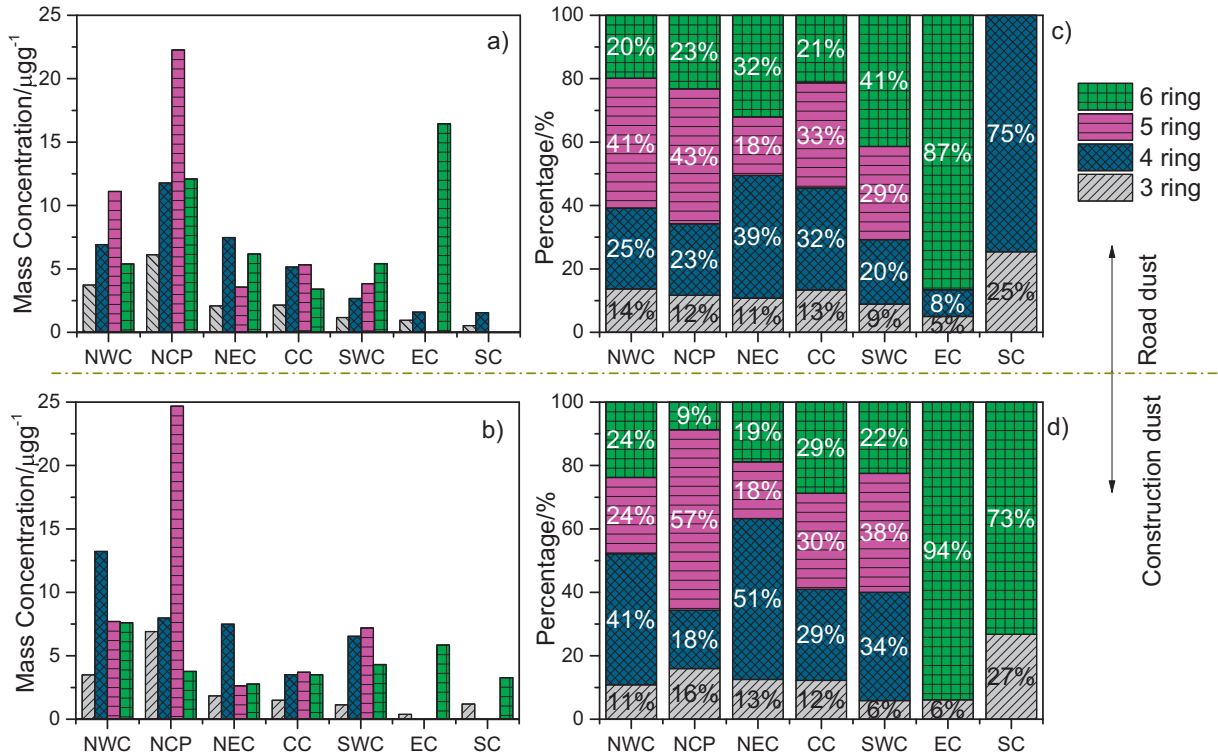


Fig. 4. Distribution of PAHs for road and construction dusts according to number of aromatic rings: a) and b) show the mass concentrations, and c) and d) show the mass percentages.

\sum PAHs_{RD} in NWC, NCP, NEC, and CC, and 87% in EC. In EC, six-rings PAHs were much prevalent than the cumulative three-to-five-rings PAHs, possibly due to more pyrogenic origins (Kong et al., 2013; De Luca et al., 2005). For CD, the proportion of four-ring PAHs was 51% in NEC, indicating significant semi-volatile partition in both gas and particle phases (Kong et al., 2015). It was noted that the proportion of three-rings PAHs was abundance in SC, 25% and 27% of \sum PAHs_{RD} and \sum PAHs_{CD}, respectively. Previous studies reported that less than three-rings PAHs are petrogenic (i.e., emitted from petroleum and its products) and susceptible to long-range atmospheric transport (Chen and Chen, 2011; Zhang et al., 2007).

A ratio of low molecular weight (LMW, three- and four-rings) to high molecular weight (HMW, five and six-rings) (abbreviated as L/H) was used to distinguish the dominance of pollution sources (Zakaria et al., 2002; Kong et al., 2013; De Luca et al., 2005). The L/H for RD and CD ranged from 0.14 to 1 and 0.06 to 1.1, respectively. The values suggest considerable variation of sources for urban fugitive dust PAHs among the Chinese cities. For RD, lower L/H was observed in SWC (0.4) and EC (0.14) due to higher pyrogenic contribution from incomplete combustion of organic matter (e.g., coal, petroleum, and wood) in industrial operations (e.g., smelting) and garbage incineration. In contrast, the L/H for RD in NWC and NCP were 0.63 and 0.53, suggesting a mixture of pyrogenic and petrogenic sources, constant with those of the coal-based industrial city of Ordos, China (0.57) (Wu et al., 2014) and mixed vehicle emission sources (0.53) (Kong et al., 2013). Higher L/H for RD were seen in NEC (1.0) and CC (0.82). In these regions, the high concentrations of LMW PAHs might be resulted from the emissions of industrial boilers (0.81) and coal-fired power plant (1.0) (Kong et al., 2013). In most of the regions, the L/H for CD were similar to those of RD samples, indicating interaction between the dust types. In NWC, however, the L/H for CD was beyond unity and approximately two times of that for RD. Petrogenic input was thus a major PAHs contamination contributor for CD in NWC.

3.4. Source identification by PAHs diagnostic ratios

The origins of PAHs in urban fugitive dust PM_{2.5} can be identified using diagnostic ratios of PAHs (Tobiszewski and Namieśnik, 2012; Yunker et al., 2002). Table 1 lists and compares the diagnostic ratios for RD and CD samples collected in different regions in this study. In short, Fla/(Fla + Pyr), Ant/(Ant + Phe), and BaA/(BaA + Chr) are three diagnostic ratios applied to distinguish the contributions of petrogenic and pyrogenic sources. The values ≤ 0.4 , < 0.1 and < 0.2 of Fla/(Fla + Pyr), Ant/(Ant + Phe), and BaA/(BaA + Chr) respectively indicated the presence of petroleum sources, whereas the values > 0.4 , > 0.1 , and > 0.37 of Fla/(Fla + Pyr), Ant/(Ant + Phe), and BaA/(BaA + Chr) respectively represented pyrolytic origins. The typical ranges for particular sources were shown in Table 1 in detail.

Among the RD samples, the ratios of Fla/(Fla + Pyr) in NWC and NEC were 0.473 and 0.447, respectively, implying that petrogenic combustion was the major source of RD PAHs in these two regions. However, Ant/(Ant + Phe) in the NEC's RD sample was 0.068, suggesting that pyrolytic sources also had some extents of contribution. Conversely, the Fla/(Fla + Pyr) ratios in NCP, CC, and SWC were > 0.5 , suggesting great influences from burnings of biomass and coal materials such as lignite, hard coal briquettes, wood and grass (Yunker et al., 2002). These results were reinforced with the BaA/(BaA + Chr) ratios, which were > 0.1 in NCP and SWC. The highest Fla/(Fla + Pyr) ratio was seen in SC (0.78), implying a strong diesel-related source (Sicre et al., 1987). For CD samples, the average Fla/(Fla + Pyr) in NWC, NCP, NEC, and CC were all approximately 0.5, emphasizing that the CD PAHs were mainly derived from gasoline combustion. However, the high Fla/(Fla + Pyr) value (0.63) in SWC indicates the predominance of diesel-combustion source.

The BaP/(BaP + Chr) for the RD and CD samples ranged from 0.06 to 0.58, slightly boarder than that for resuspended dusts collected in eastern Europe (Armstrong et al., 2004). This can be ascribed with a more complicated pollution sources for PAHs in China. The values in NEC

Table 1
Diagnostic ratios of PAHs for road and construction dusts in China and comparison of typical reported values for source identification.

Sources/sites	Sample type	BaP/(BaP + Chr)	BaP/BghiP	Fla/(Fla + Pyr)	Ant/(Ant + Phe)	BaA/(BaA + Chr)	References
Urban fugitive dust							
NWC	Road dust	0.462	0.661	0.473	/	0.235	This study
NCP		0.575	0.406	0.521	0.422	0.342	
NEC		0.180	0.130	0.447	0.068	0.209	
CC		/	/	0.573	/	0.429	
SWC		0.292	0.111	0.513	0.326	/	
EC		/	/	/	/	0.500	
SC		/	/	0.778	/	0.394	
NWC	Construction dust	0.099	0.148	0.509	/	0.189	
NCP		0.063	0.126	0.524	0.178	0.134	
NEC		/	/	0.480	/	0.103	
CC		0.489	0.171	0.525	/	0.502	
SWC		0.290	0.318	0.632	0.296	0.127	
EC		0.375	0.334	/	/	/	
SC		/	/	/	/	/	
Typical PAHs sources							
Pyrolytic					< 0.1	> 0.37	a
Petrogenic				0.400	> 0.1	< 0.2	b, c
City center street (Eastern Europe)	PM ₁₀ /PM _{2.5} - resuspended dust	0.08–0.36	0.39–0.68	0.46–0.55		0.04–0.34	d
Lignite and brown coal	Biomass and coal burning			0.59–0.85	0.00–0.16	0.39–0.49	e, f
Hard coal briquettes/coal tar				0.52–0.62	0.180	0.30–0.54	g, h
Wood/grasses combustion				0.41–0.67	0.13–0.29	0.27–0.58	i
Steel factory	Coke making, sintering plant, blast furnace and steel making		0.51–2.10	0.41–0.76		0.33–0.64	j
Diesel	Liquid fossil fuel combustion	$> 1^k$	0.45–0.83 ^l	0.6–0.7	0.11	0.18–0.69	m
Gasoline		$< 0.4^k$		0.20–0.58	0.06–0.27	0.23–0.89	n, l
Cement production		0.3–0.4		0.4–0.5			o
Industrial furnaces				0.21–0.26			p

a Kong et al., 2015; b, c, d, Martuzevicius et al., 2011; e, Grimmer et al., 1983; f, Oros and Simoneit, 2000; g, Ratajczak et al., 1984; h, Grimmer et al., 1985; i, Jenkins et al., 1996; j, Khaparde et al., 2016; k, Caricchia et al., 1999; l, Rogge et al., 1993; m, Yunker et al., 2002; n, Li and Kamens, 1993; o, Tobiszewski and Namieśnik, 2012; p, Yang et al., 1998.

Table 2
Risks of cancer for human exposure on urban road dusts in this study.

Region	Value	TEQ	Adult				Child			
			ILCR-ingestion	ILCR-dermal	ILCR-inhalation	Cancer risk	ILCR-ingestion	ILCR-dermal	ILCR-inhalation	Cancer risk
Road dust										
NWC	Mean	3.49	2.25E-04	1.19E-05	5.20E-10	2.37E-04	8.59E-06	4.28E-05	6.63E-10	5.14E-05
NCP	Mean	4.03	2.60E-04	1.38E-05	6.00E-10	2.74E-04	9.91E-06	4.94E-05	7.65E-10	5.93E-05
NEC	Mean	0.91	5.89E-05	3.12E-06	1.36E-10	6.20E-05	2.25E-06	1.12E-05	1.74E-10	1.35E-05
CC	Mean	0.46	2.97E-05	1.58E-06	6.87E-11	3.13E-05	1.13E-06	5.66E-06	8.76E-11	6.79E-06
SWC	Mean	0.52	3.34E-05	1.77E-06	7.72E-11	3.52E-05	1.27E-06	6.36E-06	9.85E-11	7.63E-06
EC	Mean	0.37	2.39E-05	1.26E-06	5.51E-11	2.51E-05	9.10E-07	4.54E-06	7.03E-11	5.45E-06
SC	Mean	0.05	3.19E-06	1.69E-07	7.37E-12	3.36E-06	1.22E-07	6.07E-07	9.39E-12	7.28E-07

and SWC's RD samples were <0.4, suggesting that gasoline combustion was the main traffic-related source (Li and Kamens, 1993; Rogge et al., 1993). In addition, the ratios in NWC and NCP were >0.4, implying the predominance of diesel emissions (Caricchia et al., 1999; Rogge et al., 1993; Yunker et al., 2002). Both CD samples collected at CC, SWC, and EC exhibited BaP/(BaP + Chr) values of 0.3–0.4. The range demonstrates that the PAHs were potentially emitted during cement production since the factories located in these cities (Manoli et al., 2004; Tobiszewski and Namieśnik, 2012). Overall, the BaA/(BaA + Chr) in the present study varied from 0.13 to 0.50, summarizing that both coal, wood, grass, and liquid fossil fuel combustions are widely pollution sources in China. It should be noted that BaA/(BaA + Chr) of >0.2 was considered a marker for multiple sources—gasoline combustion, coal and biomass burning, and steel production, whereas a value of 0.1 or below indicate influences from petroleum (Yunker et al., 2002). Its range of 0.209–0.500 was obtained for RD, whereas a much lower average of approximately 0.1 for CD. The high BaA/(BaA + Chr) ratios were consistent to the fact that the RD were influenced by combustion sources, while the CD was dominated by petroleum (Yunker et al., 2002).

3.5. Health risk assessment

The high abundances of COM-PAHs for RD and CD PM_{2.5} in NCP and NWC emphasize high potential health risks in these regions. To determine the age-specific cancer risks from exposure to environmental PAHs, the estimated BaP_{TEQ}, ILCR, and cancer risk for adults and children in the seven regions were calculated, and the results are tabulated in Table 2. In this study, the average BaP_{TEQ} for RD in the seven regions was 1.40 μg·g⁻¹, slightly higher than the average BaP_{TEQ} for CD of 1.22 μg·g⁻¹. In most of the regions, the BaP_{TEQ} values exhibited >0.1 μg·g⁻¹, indicating high carcinogenicity in the urban dust of among these Chinese cities.

A probabilistic risk assessment framework was applied to compare cancer risk from exposure to PAHs for RD and CD through direct ingestion, dermal contact, and inhalation (Table 2) (Iwegbue and Obi, 2016; Wang et al., 2011). The total RD-related cancer risk ranged from 3.36 × 10⁻⁶ to 2.74 × 10⁻⁴ for adults, and 7.28 × 10⁻⁷ to 5.93 × 10⁻⁵ for children. A total RD-related cancer risks of 10⁻⁶ to 10⁻⁴ are defined as potential health risk, whereas the risk below 10⁻⁶ suggests virtual

safety (NYS DOH, 2007). Hence, the high RD-related cancer risk in this study should be an alert for adults. Regarding to individual ILCRs, dermal contact and ingestion are the main contributors to cancer risk for adults, while ingestion is the key pathway for children. The risks for both adults and children are mainly induced by frequent hand-to-mouth activity whereby RD can be readily ingested. For CD, the adult cancer risks ranged from 4.27 × 10⁻⁶ to 1.89 × 10⁻⁴, 2.26 × 10⁻⁷ to 1.10 × 10⁻⁶, and 9.86 × 10⁻¹² to 4.37 × 10⁻⁶ for exposure through ingestion, dermal contact, and inhalation, respectively. For children, dermal exposure to CD exhibited the highest risk, followed by ingestion and inhalation. The total CD-related cancer risk for adults was higher than the acceptable level of 10⁻⁶ (i.e., one cancer case per one million people), which is approximately 10 times higher than that for children. The total CD-related cancer risk for adults was the highest (approximately 10⁻⁴) in most north regions (i.e., NCP, SWC, and NWC), followed by NEC and CC (10⁻⁵), and EC and SC (10⁻⁶). The results of the present study indicated that exposure to RD from construction sources represents a potential risk of cancer for Chinese residents (Table 3).

4. Conclusion

The present study proves the high abundances of PAHs in urban fugitive dusts in the seven regions in China. The five-to-six-rings PAHs comprised a significant proportion of RD, and four-rings PAHs were prevalent in CD, indicating that pyrogenic sources were main contributors to PAHs. The PAHs levels varied substantially across the regions in relation to local and regional pollution sources. The highest ∑PAHs_{RD} and ∑PAHs_{CD} were found in NCP, 10 times higher than those in SC. In comparison, the PAHs for RD in the northern regions show higher levels of COM-PAHs than southern regions because of the intensive industrial activities in northern China. The source characterization using diagnostic ratios, additional with CoD analysis, demonstrate that the emissions from vehicles, coal combustion and biomass burning were the major sources of PAHs for RD, while industrial emissions comprised a substantial fraction of CD. The BaP_{TEQ} for RD and CD both show higher values in northern and central China, in accordance with the geographic distribution of PAHs levels. The total RD- and CD-related cancer risks for adults were higher than those for children. The results of this study offer a critical overview on the severe pollutions on PAHs for urban fugitive dusts, particularly in northern regions.

Table 3
Risks of cancer for human exposure on urban construction dusts in this study.

Region	Value	TEQ	Adult				Child			
			ILCR-ingestion	ILCR-dermal	ILCR-inhalation	Cancer risk	ILCR-ingestion	ILCR-dermal	ILCR-inhalation	Cancer risk
Construction dust										
NWC	Mean	1.50	9.69E-05	5.13E-06	2.24E-10	1.02E-04	3.70E-06	1.84E-05	2.85E-10	2.21E-05
NCP	Mean	2.94	1.89E-04	1.00E-05	4.37E-10	1.99E-04	7.22E-06	3.60E-05	5.58E-10	4.32E-05
NEC	Mean	0.52	3.33E-05	1.76E-06	7.69E-11	3.51E-05	1.27E-06	6.33E-06	9.81E-11	7.60E-06
CC	Mean	0.88	5.68E-05	3.01E-06	1.31E-10	5.98E-05	2.17E-06	1.08E-05	1.67E-10	1.30E-05
SWC	Mean	2.56	1.65E-04	8.74E-06	3.81E-10	1.74E-04	6.29E-06	3.14E-05	4.86E-10	3.77E-05
EC	Mean	0.06	3.78E-06	2.00E-07	8.73E-12	3.98E-06	1.44E-07	7.19E-07	1.11E-11	8.63E-07
SC	Mean	0.07	4.27E-06	2.26E-07	9.86E-12	4.50E-06	1.63E-07	8.12E-07	1.26E-11	9.75E-07

Supplementary data to this article can be found online at <https://doi.org/10.1016/j.scitotenv.2019.06.099>.

Acknowledgment

This research is supported by the National Project of Causes and Treatment of Heavy Air Pollution (DQGG0105-01); Ministry of Science and Technology of the People's Republic of China (2013FY112700), a grant from SKLLQG, Chinese Academy of Sciences (SKLLQG1616).

References

- Agarwal, T., Khillare, P., Shridhar, V., Ray, S., 2009. Pattern, sources and toxic potential of PAHs in the agricultural soils of Delhi, India. *J. Hazard. Mater.* 163, 1033–1039.
- Ajmone-Marsan, F., Biasioli, M., Kralj, T., Grčman, H., Davidson, C.M., Hursthouse, A.S., Madrid, L., Rodrigues, S., 2008. Metals in particle-size fractions of the soils of five European cities. *Environ. Pollut.* 152, 73–81.
- Amato, F., Pandolfi, M., Moreno, T., Furger, M., Pey, J., Alastuey, A., Bukowiecki, N., Prevot, A.S.H., Baltensperger, U., Querol, X., 2011. Sources and variability of inhalable road dust particles in three European cities. *Atmos. Environ.* 45, 6777–6787.
- Armstrong, B., Hutchinson, E., Unwin, J., Fletcher, T., 2004. Lung cancer risk after exposure to polycyclic aromatic hydrocarbons: a review and meta-analysis. *Environ. Health Persp.* 112, 970.
- Bhaskar, V.S., Sharma, M., 2008. Assessment of fugitive road dust emissions in Kanpur, India. A note. *Transp. Environ. Res. Part D: Transp. Environ.* 13, 400–403.
- Bin Abas, M.R., Simoneit, B.R., Elias, V., Cabral, J., Cardoso, J., 1995. Composition of higher molecular weight organic matter in smoke aerosol from biomass combustion in Amazonia. *Chemos* 30, 995–1015.
- Cao, J.J., Chow, J.C., Watson, J.G., Wu, F., Han, Y.M., Jin, Z.D., Shen, Z.X., An, Z.S., 2008. Size-differentiated source profiles for fugitive dust in the Chinese Loess Plateau. *Atmos. Environ.* 42, 2261–2275.
- Cao, J.J., Shen, Z.X., Chow, J.C., Watson, J.G., Lee, S., Tie, X.X., Ho, K.F., Wang, G.H., Han, Y., 2012. Winter and summer PM_{2.5} chemical compositions in fourteen Chinese cities. *J. Air & Waste Manage. Assoc.* 62, 1214–1226.
- Caricchia, A.M., Chiavarini, S., Pezza, M., 1999. Polycyclic aromatic hydrocarbons in the urban atmospheric particulate matter in the city of Naples (Italy). *Atmos. Environ.* 33 (23), 3731–3738.
- Chen, C.W., Chen, C.F., 2011. Distribution, origin, and potential toxicological significance of polycyclic aromatic hydrocarbons (PAHs) in sediments of Kaohsiung Harbor, Taiwan. *Mar. Pollut. Bull.* 63, 417–423.
- Chen, L.W.A., Watson, J.G., Chow, J.C., Magliano, K.L., 2007. Quantifying PM_{2.5} source contributions for the San Joaquin Valley with multivariate receptor models. *Environ. Sci. Technol.* 41, 2818–2826.
- Chen, Y., Cao, J., Zhao, J., Xu, H., Arimoto, R., Wang, G., Han, Y., Shen, Z., Li, G., 2014. n-Alkanes and polycyclic aromatic hydrocarbons in total suspended particulates from the southeastern Tibetan Plateau: concentrations, seasonal variations, and sources. *Sci. Total Environ.* 470, 9–18.
- De Luca, G., Furesi, A., Micera, G., Panzanelli, A., Piu, P.C., Pilo, M.I., Spano, N., Sanna, G., 2005. Nature, distribution and origin of polycyclic aromatic hydrocarbons (PAHs) in the sediments of Olbia harbor (Northern Sardinia, Italy). *Mar. Pollut. Bull.* 50, 1223–1232.
- Diego, I., Pelegrí, A., Torno, S., Torano, J., Menendez, M., 2009. Simultaneous CFD evaluation of wind flow and dust emission in open storage piles. *Applied Math. Model.* 33, 3197–3207.
- Diggs, D.L., Huderson, A.C., Harris, K.L., Myers, J.N., Banks, L.D., Rekhadevi, P.V., Niaz, M.S., Ramesh, A., 2011. Polycyclic aromatic hydrocarbons and digestive tract cancers: a perspective. *J. Environ. Sci. Health, Part C* 29, 324–357.
- Durant, J.L., Busby, J.W., Lafleur, A.L., Penman, B.W., Crespi, C.L., 1996. Human cell mutagenicity of oxygenated, nitrated and unsubstituted polycyclic aromatic hydrocarbons associated with urban aerosols. *Mutat. Res. Genet. Toxicol.* 371, 123–157.
- Grimmer, G., Jacob, J., Naujack, K.W., Dettbarn, G., 1983. Determination of polycyclic aromatic compounds emitted from brown-coal-fired residential stoves by gas chromatography/mass spectrometry. *Anal. Chem.* 55, 892–900.
- Grimmer, G., Jacob, J., Dettbarn, G., Naujack, K.W., 1985. Determination of polycyclic aromatic compounds, azaarenes, and thiaarenes emitted from coal-fired residential furnaces by gas chromatography/mass spectrometry. *Fresen. Z. Anal. Chem.* 322, 595–602.
- Han, B., Bai, Z., Guo, G., Wang, F., Li, F., Liu, Q., Ji, Y., Li, X., Hu, Y., 2009. Characterization of PM₁₀ fraction of road dust for polycyclic aromatic hydrocarbons (PAHs) from Anshan, China. *J. Hazard. Mater.* 170, 934–940.
- Hussain, K., Rahman, M., Prakash, A., Hoque, R.R., 2015. Street dust bound PAHs, carbon and heavy metals in Guwahati city-seasonality, toxicity and sources. *Sustain. Cities Soc.* 19, 17–25.
- Iwegbue, C.M., Obi, G., 2016. Distribution, sources, and health risk assessment of polycyclic aromatic hydrocarbons in dust from urban environment in the Niger Delta, Nigeria. *Hum. Ecol. Risk Assess.* 22, 623–638, 2016.
- Jang, E., Alam, M.S., Harrison, R.M., 2013. Source apportionment of polycyclic aromatic hydrocarbons in urban air using positive matrix factorization and spatial distribution analysis. *Atmos. Environ.* 79, 271–285.
- Jenkins, B.M., Jones, A.D., Turn, S.Q., Williams, R.B., 1996. Emission factors for polycyclic aromatic hydrocarbons from biomass burning. *Environ. Sci. Technol.* 30, 2462–2469.
- Khapharde, V.V., Bhanarkar, A.D., Majumdar, D., Rao, C.C., 2016. Characterization of polycyclic aromatic hydrocarbons in fugitive PM₁₀ emissions from an integrated iron and steel plant. *Sci. Total Environ.* 562, 155–163.
- Kim, K.H., Jahan, S.A., Kabir, E., Brown, R.J., 2013. A review of airborne polycyclic aromatic hydrocarbons (PAHs) and their human health effects. *Environ. Inter.* 60, 71–80.
- Kong, S., Ji, Y., Li, Z., Lu, B., Bai, Z., 2013. Emission and profile characteristic of polycyclic aromatic hydrocarbons in PM_{2.5} and PM₁₀ from stationary sources based on dilution sampling. *Atmos. Environ.* 77, 155–165.
- Kong, S., Li, X., Li, Q., Yin, Y., Li, L., Chen, K., Liu, D., Yuan, L., Pang, X., 2015. Subway construction activity influence on polycyclic aromatic hydrocarbons in fine particles: comparison with a background mountainous site. *Atmos. Res.* 161, 82–92.
- Lannerö, E., Wickman, M., van Hage, M., Bergström, A., Pershagen, G., Nordvall, L., 2008. Exposure to environmental tobacco smoke and sensitisation in children. *Thorax* 63, 172–176.
- Lee, B.K., Dong, T.T., 2011. Toxicity and source assignment of polycyclic aromatic hydrocarbons in road dust from urban residential and industrial areas in a typical industrial city in Korea. *J. Mater. Cycles Waste* 13, 34–42.
- Li, C.K., Kamens, R.M., 1993. The use of polycyclic aromatic hydrocarbons as source signatures in receptor modeling. *Atmos. Environ.* 27A, 523–532.
- Lima, A.L.C., Farrington, J.W., Reddy, C.M., 2005. Combustion-derived polycyclic aromatic hydrocarbons in the environment—a review. *Environ. Forensic* 6, 109–131.
- Lin, B., Wang, X., 2014. Exploring energy efficiency in China's iron and steel industry: a stochastic frontier approach. *Energy Policy* 72, 87–96.
- Majumdar, D., Rajaram, B., Meshram, S., Chalapati, R.C., 2012. PAHs in road dust: ubiquity, fate, and summary of available data. *Crit. Rev. Environ. Sci. Technol.* 42, 1191–1232.
- Manoli, E., Kouras, A., Samara, C., 2004. Profile analysis of ambient and source emitted particle-bound polycyclic aromatic hydrocarbons from three sites in northern Greece. *Chemos* 56, 867–878.
- Martuzevicius, D., Kluciniņkas, L., Prasauskas, T., Krugly, E., Kauneliene, V., Strandberg, B., 2011. Resuspension of particulate matter and PAHs from street dust. *Atmos. Environ.* 45, 310–317.
- Murakami, M., Nakajima, F., Furumai, H., 2005. Size- and density-distributions and sources of polycyclic aromatic hydrocarbons in urban road dust. *Chemos* 61 (6), 783–791.
- Netto, A.D.P., Krauss, T.M., Cunha, I.F., Rego, E.C., 2006. PAHs in SD: polycyclic aromatic hydrocarbons levels in street dust in the central area of Niterói City, RJ, Brazil. *Water, Air, Soil Pollut* 176, 57–67.
- Nisbet, I.C., Lagoy, P.K., 1992. Toxic equivalency factors (TEFs) for polycyclic aromatic hydrocarbons (PAHs). *Regul. Toxicol. Pharmacol.* 16 (3), 290–300.
- NYS DOH (New York State Department of Health), 2007. Hopewell precision area contamination: Appendix C-NYS DOH. Procedure for Evaluating Potential Health Risks for Contaminants of Concern Available at: <http://www.health.ny.gov/environmental/investigations/hopewell/appendc.htm>.
- Oros, D.R., Simoneit, B.R., 2000. Identification and emission rates of molecular tracers in coal smoke particulate matter. *Fuel* 79, 515–536.
- Peng, C., Chen, W., Liao, X., Wang, M., Ouyang, Z., Jiao, W., Bai, Y., 2011. Polycyclic aromatic hydrocarbons in urban soils of Beijing: status, sources, distribution and potential risk. *Environ. Pollut.* 159, 802–808.
- Ratajczak, E.A., Ahland, E., Grimmer, G., Diettbarn, G., 1984. Verminderung der emission von polycyclischen aromatischen kohlenwasserstoffen beim einsatz von pech durch bitumen in steinkohlenbriketts. *Staub. Reinhalt. Luft* 44, 505–509.
- Rogge, W.F., Hildemann, L.M., Mazurek, M.A., Cass, G.R., Simoneit, B.R.T., 1993. Sources of fine organic aerosol. 2. Noncatalyst and catalyst-equipped automobiles and heavy-duty diesel trucks. *Environ. Sci. Technol.* 27, 636–651.
- Rogge, W.F., Medeiros, P.M., Simoneit, B.R., 2007. Organic marker compounds in surface soils of crop fields from the San Joaquin Valley fugitive dust characterization study. *Atmos. Environ.* 41, 8183–8204.
- See, S.W., Karthikeyan, S., Balasubramanian, R., 2006. Health risk assessment of occupational exposure to particulate-phase polycyclic aromatic hydrocarbons associated with Chinese, Malay and Indian cooking. *J. Environ. Monit.* 8, 369–376.
- Shen, Z., Sun, J., Cao, J., Zhang, L., Zhang, Q., Lei, Y., Gao, J., Huang, R.J., Liu, S., Huang, Y., Zhu, C., Xu, H., Zheng, C., Liu, P., Xue, Z., 2016. Chemical profiles of urban fugitive dust PM_{2.5} samples in Northern Chinese cities. *Sci. Total Environ.* 569–570, 619–626.
- Sicre, M.A., Marty, J.C., Saliot, A., Aparicio, X., Grimalt, J., Albaiges, J., 1987. Aliphatic and aromatic hydrocarbons in different sized aerosols over the Mediterranean Sea: occurrence and origin. *Atmos. Environ.* 21, 2247–2259.
- Smith, D., Edelhofer, E., Harrison, R.M., 1995. Polynuclear aromatic hydrocarbon concentrations in road dust and soil samples collected in the United Kingdom and Pakistan. *Environ. Technol.* 16, 45–53.
- Suman, S., Sinha, A., Tarafdar, A., 2016. Polycyclic aromatic hydrocarbons (PAHs) concentration levels, pattern, source identification and soil toxicity assessment in urban traffic soil of Dhanbad, India. *Sci. Total Environ.* 545, 353–360.
- Sun, J., Shen, Z.X., Zhang, L.M., Lei, Y.L., Gong, X.S., Zhang, Q., Zhang, T., Xu, H.M., Cui, S., Wang, Q.Y., Cao, J.J., Tao, J., Zhang, N.N., Zhang, R.J., 2019. Chemical source profiles of urban fugitive dust PM_{2.5} samples from 21 cities across China. *Sci. Total Environ.* 649, 1045–1053.
- Tobiszewski, M., Namieśnik, J., 2012. PAH diagnostic ratios for the identification of pollution emission sources. *Environ. Pollut.* 162, 110–119.
- US EPA, 1993. Provisional Guidance for Quantitative Risk Assessment of PAH. US Environmental Protection Agency EPA/600/R-93/089.
- Wang, W., Huang, M.J., Kang, Y., Wang, H.S., Leung, A.O., Cheung, K.C., Wong, M.H., 2011. Polycyclic aromatic hydrocarbons (PAHs) in urban surface dust of Guangzhou, China: status, sources and human health risk assessment. *Sci. Total Environ.* 409, 4519–4527.
- Wang, X., Shen, Z.X., Liu, F.B., Lu, D., Tao, J., Lei, Y.L., Zhang, Q., Zeng, Y.L., Xu, H.M., Wu, Y.F., Zhang, R.J., Cao, J.J., 2018. Saccharides in summer and winter PM_{2.5} over Xi'an,

- Northwestern China: sources, and yearly variations of biomass burning contribution to PM_{2.5}. *Atmos. Res.* 214, 410–417.
- Wu, D., Wang, Z., Chen, J., Kong, S., Fu, X., Deng, H., Shao, G., Wu, G., 2014. Polycyclic aromatic hydrocarbons (PAHs) in atmospheric PM_{2.5} and PM₁₀ at a coal-based industrial city: implication for PAH control at industrial agglomeration regions, China. *Atmos. Res.* 149, 217–229.
- Yang, H.H., Lee, W.J., Chen, S.J., Lai, S.O., 1998. PAH emission from various industrial stacks. *J. Hazard. Mater.* 60 (2), 159–174, 1998.
- Yang, H.H., Chiang, C.F., Lee, W.J., Hwang, K.P., Wu, E.M.Y., 1999. Size distribution and dry deposition of road dust PAHs. *Environ. Int.* 25 (5), 585–597.
- Yang, H.H., Lai, S.O., Hsieh, L.T., Hsueh, H.J., Chi, T.W., 2002. Profiles of PAH emission from steel and iron industries. *Chemos* 48, 1061–1074.
- Yu, L., Wang, G., Zhang, R., Zhang, L., Sng, Y., Wu, B., Li, X., An, K., Chu, J., 2013. Characterization and source apportionment of PM_{2.5} in an urban environment in Beijing. *Aerosol Air Qual. Res.* 13, 574–583.
- Yunker, M.B., Macdonald, R.W., Vingarzan, R., Mitchell, R.H., Goyette, D., Sylvestre, S., 2002. PAHs in the Fraser River basin: a critical appraisal of PAH ratios as indicators of PAH source and composition. *Org. Geochem.* 33, 489–515.
- Zakaria, M.P., Takada, H., Tsutsumi, S., Ohno, K., Yamada, J., Kouno, E., Kumata, H., 2002. Distribution of polycyclic aromatic hydrocarbons (PAHs) in rivers and estuaries in Malaysia: a widespread input of petrogenic PAHs. *Environ. Sci. Technol.* 36, 1907–1918.
- Zeng, Y.L., Shen, Z.X., Lei, Y.L., Zhang, T., Zhang, Q., Xu, H.M., Wang, Q.Y., Cao, J.J., Yang, L., 2018. PAHs in fine particles over Xi'an, a typical northwestern city in China: sources, distribution, and controlling factors. *Environ. Sci. Proc. Impacts* 20, 1262–1272.
- Zhang, S., Zhang, Q., Darisaw, S., Ehie, O., Wang, G., 2007. Simultaneous quantification of polycyclic aromatic hydrocarbons (PAHs), polychlorinated biphenyls (PCBs), and pharmaceuticals and personal care products (PPCPs) in Mississippi river water, in New Orleans, Louisiana, USA. *Chemos* 66, 1057–1069.
- Zhang, Q., Shen, Z., Cao, J., Ho, K., Zhang, R., Bie, Z., Chang, H., Liu, S., 2014. Chemical profiles of urban fugitive dust over Xi'an in the south margin of the Loess Plateau, China. *Atmos. Pollu. Res.* 5, 421–430.